Long-tailed probability distributions in turbulent-pipe-flow mixing

J. E. Guilkey*
Department of Mechanical Engineering, University of Utah, Salt Lake City, Utah 84112

A. R. Kerstein
Combustion Research Facility, Sandia National Laboratories, Livermore, California 94551-0969

P. A. McMurtry and J. C. Klewicki
Department of Mechanical Engineering, University of Utah, Salt Lake City, Utah 84112

(Received 11 March 1997)

Exponential-tailed scalar probability density functions (PDF's) are obtained by high-pass filtering scalar concentration time series measured in turbulent pipe flow. This behavior reflects the scale separation of scalar and velocity fluctuations that develops in this flow, such that the low-wave-number scalar fluctuations act as an imposed scalar gradient stirred by finer-scale wall-generated shear. This observation broadens the class of flows in which long-tailed scalar PDF's are anticipated to occur. [S1063-651X(97)12908-7]

PACS number(s): 47.62.+q, 47.60.+i

I. INTRODUCTION

Since exponential-tailed temperature probability density functions (PDF's) were observed in the ''hard turbulence'' regime of Rayleigh convection [1], various experimental and theoretical studies have been performed in order to identify their origins. One mechanism for long-tailed PDF formation that has been identified is associated with turbulent mixing of a passive scalar subject to an imposed mean gradient [2–6]. It has not yet been established that this mechanism is operative in flows with no imposed mean gradient.

Here it is demonstrated that flows in which the length scales of the dominant scalar fluctuations and the turbulent stirring are well separated may exhibit this mechanism. It has recently been demonstrated experimentally that mixing in turbulent pipe flow leads to this type of length scale separation [7,8].

This behavior was anticipated based on analysis and computational modeling [9] that suggested the following picture. The scalar concentration field in turbulent pipe flow has low-wave-number (relative to the pipe diameter) spectral content, reflecting either the inlet conditions or nonlocal (in wave number) spectral transfer of scalar fluctuations by high-wave-number random advection. The low-wave-number fluctuations are, in effect, frozen on the time scale of high-wave-number evolution, except that the wave-number range of the frozen fluctuations is gradually eroded from above by turbulent eddy diffusion. Eddy diffusion is driven by wall shear, so its characteristic length scale is the pipe diameter.

As this process evolves, significant scale separation develops between the stirring scale (the pipe diameter) and the scale range of the frozen low-wave-number fluctuations. The wave-number interval between the stirring scale and the frozen range is denoted the equilibrium range, reflecting the kinematics of scalar evolution in that range [9]. In the equilibrium range, turbulent stirring induces a scalar cascade to higher wave numbers (albeit with significant backscatter that leads to nonstandard spectral scaling).

The relevant point here is that stirring length and time scales are much smaller than the corresponding scales of the dominant scalar fluctuations. Therefore scalar evolution as seen at the stirring scale is analogous to mixing in an imposed scalar gradient.

Even if this analogy is valid locally, it is not obvious that ensemble-averaged scalar statistics will reflect the mechanism of long-tailed PDF formation in the presence of an imposed mean gradient. The dominant scalar fluctuations are at low wave numbers that see no imposed gradient. Here, scalar time series measured in turbulent pipe flow are high-pass filtered in order to ascertain whether the fine-scale fluctuations superimposed on the dominant large-scale fluctuations exhibit non-Gaussian statistics of the type found for scalar fluctuations in the presence of an imposed mean gradient.

II. EXPERIMENTAL CONFIGURATION

The experimental facility has a 9.75 m long test section consisting of eight 1.22 m sections of 25 mm I.D. quartz pipe, for a total length to diameter ratio of about 390. The quartz sections are connected by brass couplers each of which is fitted with a pressure tap and constructed so as to give a smooth section to section transition. A reservoir, pump, return section, and flowmeter complete the flow facility. Total fluid volume of the facility is about 35 l. The passive scalar used in each experiment is fluorescent dye. For each of the experiments the Reynolds number based on mean velocity and the pipe diameter is 7500.

Two separate experiments, which vary only in inlet condition, are described here. The first of these, experiment 1, includes a 1.33 m section of 25.4 mm diameter PVC pipe that was divided in half along its entire length by a 1.59 mm thick piece of PVC, which was tapered to a point at the trailing edge. This device, shown in Fig. 1, replaced the second quartz section so that the main flow was divided upon

*Electronic address: guilkey@akeila.mech.utah.edu

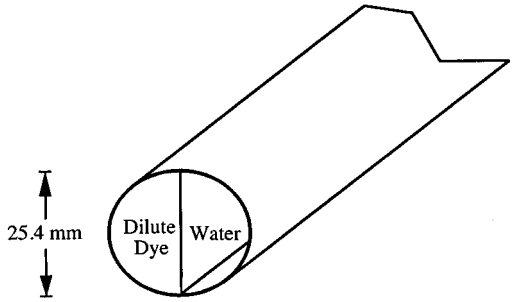

FIG. 1. Schematic of the partitioned pipe inlet (experiment 1).

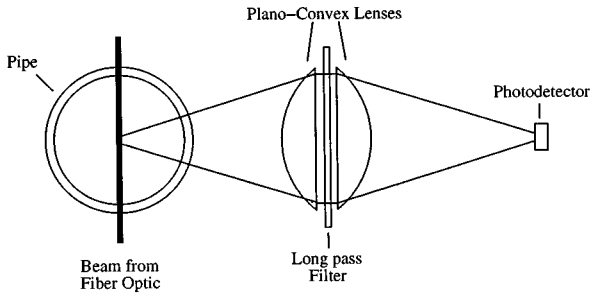

FIG. 3. Optical configuration of the scalar interrogation location.

entering the mixing region of the pipe. On one side of the divided pipe, dilute fluorescent dye was injected at a rate of approximately 1 l/min using a constant head reservoir located 1.4 m above the test section. For the initialization of experiment 2, the main flow is divided at a ''T'' into two straight sections. At the entrance of one of these sections, dilute fluorescent dye was injected into one stream at a rate of approximately 1 l/min from a constant head reservoir. The two streams were recombined through a second ''T'' junction, as shown in Fig. 2. The entire device was constructed of 25.4 mm diameter PVC.

In both experiments the scalar field is interrogated at 7 downstream locations using the 488 nm (1.5 W continuous wave) line from an argon ion laser. The single beam out of the laser is focused into a custom built fiber optic bundle, each leg of which is terminated at a different downstream location. The configuration used is shown schematically in Fig. 3. A low-pass filter is used to attenuate the scattered laser light while passing the longer wavelength fluorescent light. The filter is positioned between two planoconvex lenses causing the light to be at normal incidence upon the filter. This is the condition for which the filter is designed and thus performs best. The measurement system allows the interrogation of a single point on the center line of the pipe at each axial location. For the given flow speed, the signal from each photodetector was sampled at 1000 Hz for up to 120 secs which is approximately the time required for the fluid to make a complete loop. Sampling was achieved with an eight-channel, 16-bit A/D converter interfaced with a UNIX workstation.

The Schmidt number for the dye in the fluid is about 1900 [10] ($Sc=\nu/D_m$) where D_m is the molecular diffusivity of fluorescein in water. The Kolmogorov length scale, $\eta=(\epsilon/\nu^3)^{1/4}$, was estimated as $\eta=0.18$ mm at the center line of the pipe, calculated using an estimate of the dissipation rate ϵ, as reported by Lawn [11]. This corresponds to a Kolmogorov frequency of about 266 Hz ($f_k=U/2\pi\eta$). Thus, the sampling rate is well above the Nyquist criterion for resolving the smallest features of the flow field. The factor limiting the resolution of the small structure of the flow was the size of the beam from the fiber optic which is about 2 mm in diameter, or about 10 Kolmogorov scales. While this limits the ability to resolve the smallest scale features of the scalar field, the resolution is more than adequate to achieve the objectives of the present research.

III. EXPERIMENTAL RESULTS

Scalar spectra from experiments 1 and 2 are shown in Figs. 4 and 5(a), respectively, at five downstream locations. A substantial difference in the spectral content from each experiment is readily apparent. Namely, the spectra from experiment 1 are relatively flat in shape in the region extending from the lowest wave number to the wave number corresponding to the pipe diameter ($K=1$). This is in contrast to

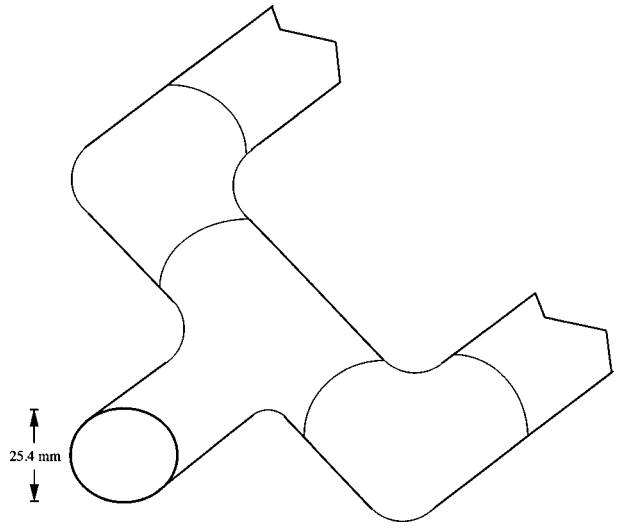

FIG. 2. Schematic of the ''T'' junction inlet (experiment 2).

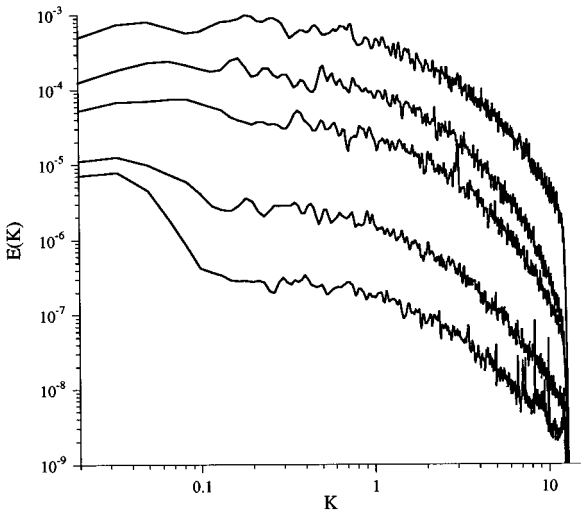

FIG. 4. Power spectral densities of scalar fluctuations, experiment 1. Axial locations (from top to bottom) are $x/D=30.0$, 44.2, 58.4, 84.3, and 109.2, where D is the pipe diameter.

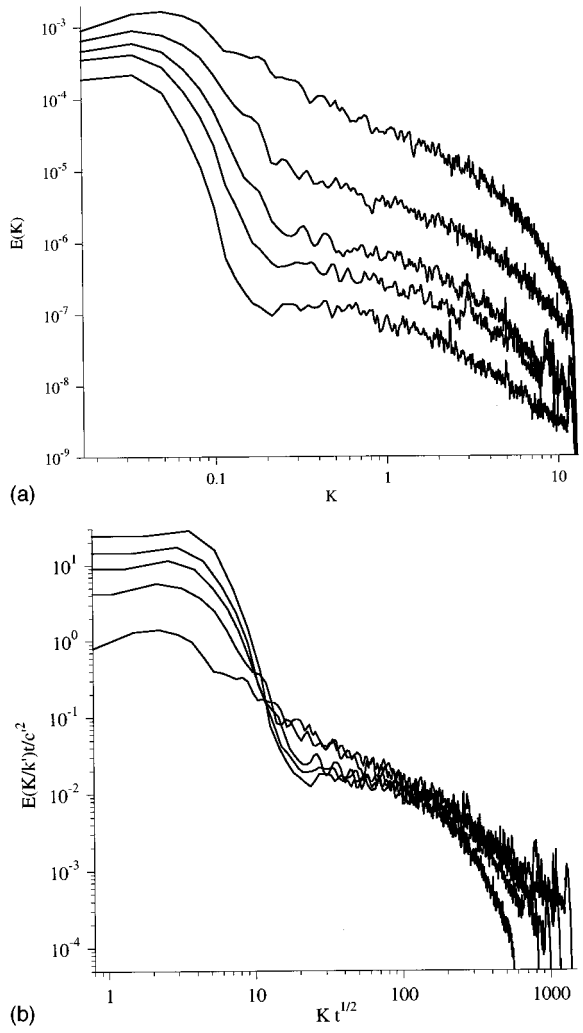

FIG. 5. (a) Power spectral densities of scalar fluctuations, experiment 2. Axial locations (from top to bottom) are $x/D=20.5$, 36.0, 50.2, 64.4, and 90.3. (b) Spectra subject to ''equilibrium'' range scalings, indicating self-preserving behavior.

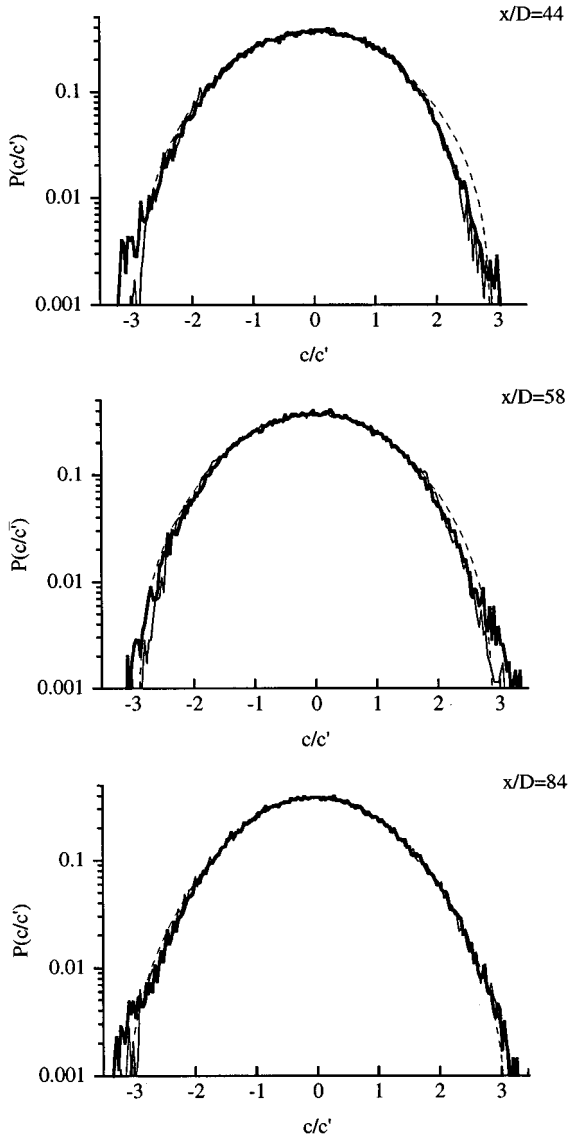

FIG. 6. PDF's of unfiltered (thin line) and high-pass-filtered (thick line) data at three streamwise locations (experiment 1). Dashed line indicates a Gaussian curve fit to the unfiltered data.

the spectra from experiment 2 which are dominated by a low-wave-number component that is approximately 3 orders of magnitude greater than the value of the spectra at $K=1$. The substantial difference in the shape of the low-K spectra is governed by the geometric differences in the scalar initialization process. The dominant low-K fluctuations in experiment 2 are attributed to natural fluctuations in velocity and pressure resulting from the two streams meeting in the ''T'' junction. In this case, small pressure fluctuations in the incoming streams can result in periodically varying contributions to the main pipe flow from the two streams. In both cases the spectra at $K>1$ approximately obey a typical inertial-range decay. Note that the low-wave-number spectra from experiment 2 do not quite reflect the description of being ''frozen'' as discussed in the Introduction. However, the decay of the low-wave-number fluctuations is occuring at a rate that is slower than other relevant flow evolution processes. It is suspected that this decay in the level of the low-wave-number tail is due to interactions of near-wall and core-region fluid, rather than low-wave-number axial mixing.

When the data of Fig. 5(a) are scaled vertically by t/c'^2 and horizontally by $t^{1/2}$, a collapse is seen in the ''equilibrium'' region which bridges the low-K portion of the spectrum with the inertial range [Fig. 5(b)]. That these scalings are obeyed is indicative of a self-preserving scalar field in which the amplitude of the equilibrium region is determined by a balance of spectral intensity moving to the low-K and inertial range portions of the spectrum. A complete description of the scalar spectra and the factors influencing their shape can be found in Guilkey *et al.* [7,8].

The scalar time series are high-pass filtered in order to remove the low-wave-number fluctuations. The wave-number cutoff for the filter was generally chosen to be near the beginning of the equilibrium range (i.e., $K=0.27$). For both of the experiments the PDF's of the unfiltered data were approximately Gaussian.

The assertion that clearcut length scale separation between the dominant fluctuations and the stirring scale is needed in order to see behavior associated with an imposed scalar gradient implies that such behavior should not be ob-

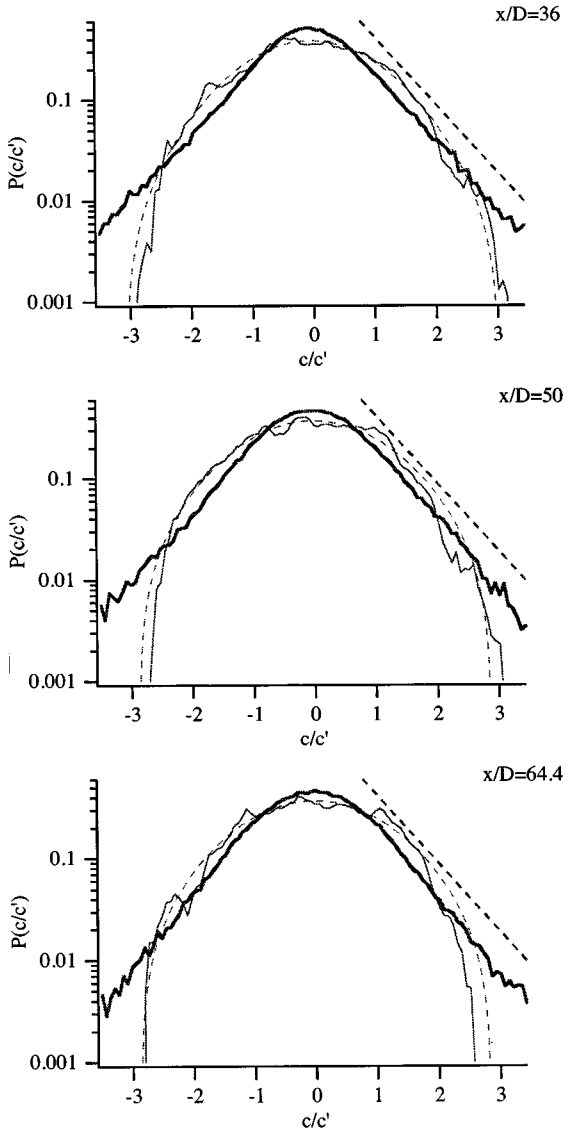

FIG. 7. PDF's of unfiltered (thin line) and high-pass-filtered (thick line) data at three streamwise locations (experiment 2). Dashed lines indicates a Gaussian curve fit to the unfiltered data and a line of exponential decay for comparison.

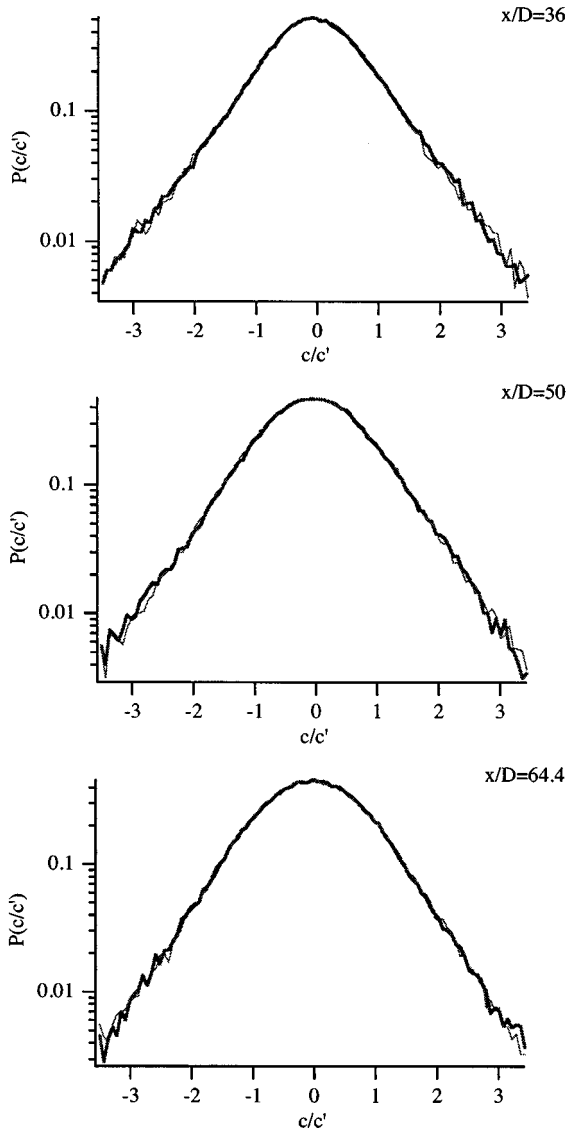

FIG. 8. PDF's of data subject to different filter cutoffs (experiment 2). The thick line is for a cutoff wave number of $K=0.27$ and the thin line is for a cutoff wave number of $K=0.74$.

served in the PDF's of the data from experiment 1. Figure 6 bears out that expectation. This figure shows plots of the PDF of the unfiltered data (thin line), the high-pass-filtered data (thick line), and a Gaussian curve fit to the unfiltered data (dashed line). Each of these is shown for three different streamwise locations, $x/D=44$, 58.4, and 84.3, where D is the pipe diameter. The filtered and unfiltered PDF's are essentially indistinguishable, and both are fit relatively well by a Gaussian distribution in the tails as well as in the central region.

PDF's from experiment 2, where the scalar spectral intensity is predominantly at wave numbers well below the stirring wave number, show much different behavior. Figure 7 shows PDF's from three locations, $x/D=36$, 50, and 64.4. Each plot contains the PDF of the data before being high-pass filtered (thin line), a Gaussian curve fit to the unfiltered PDF (dashed line), the PDF of the high-pass-filtered data (thick line) and a line indicating an exponential decay (thick dashed line). This last line is not a curve fit; its presence is merely intended as a comparison. The PDF's of the high-pass-filtered data are seen to approach the anticipated exponential form. The data from the same three axial positions are again presented in Fig. 8. Here, both lines indicate data which have been high-pass filtered at different cutoff wave numbers, $K=0.27$ (thick line) and $K=0.74$ (thin line). These graphs indicate that the shape of the filtered PDF is invariant with respect to cutoff wave number provided that the cutoff is within the equilibrium range. Figure 9 shows the high-pass-filtered PDF from each interrogation location. (Each PDF has been shifted one decade vertically with respect to the previous one.) The exponential form of the tails is maintained until at least $x/D=90.3$. Beyond that, it is likely that the transition back to a more Gaussian shape is due to a low signal-to-noise ratio at the far downstream positions. In Fig. 10, the first five of these PDF's are plotted without the vertical displacements. The collapse of the PDF's of c/c', where c'^2 is the variance of c, indicates self-similarity of the

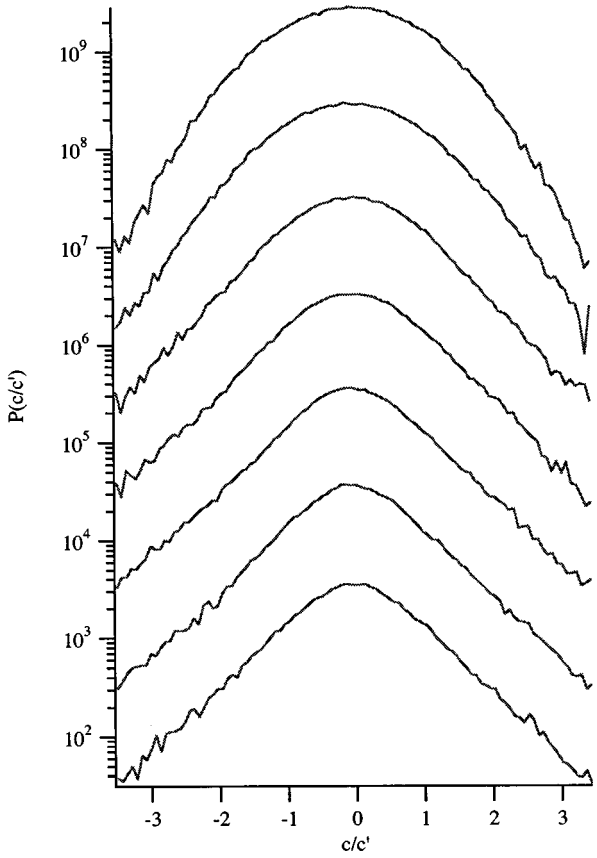

FIG. 9. PDF's of high-pass-filtered ($K=0.27$) data (experiment 2). Each PDF is offset vertically by one decade with respect to the previous one. Axial locations (from bottom to top) are $x/D=20.5$, 36.0, 50.2, 64.4, 90.3, 115.2, and 147.0. Exponential tails persist until $x/D=90.3$, beyond which the signal-to-noise ratio is probably not adequate to observe that behavior.

high-pass-filtered scalar fluctuations. A small deviation from a perfect collapse exists as evidenced by the dashed curves which represent the PDF's of the two farthest downstream positions. In general the PDF's become slightly more blunt with increasing axial location. It is unclear if this is a result of a decreasing signal-to-noise ratio or an increasingly favorable imposed gradient condition.

The difference in the behavior of the PDF from experiment 2 to experiment 1 reinforces the hypothesis that large-amplitude low-wave-number fluctuations, well separated in scale from the stirring scale, act as an imposed scalar gradient. Even in experiment 1, however, a low-wave-number component develops in the very far field, but the behavior of the PDF seen in experiment 2 is never exhibited. This is most likely due to the low signal-to-noise ratio at the far-field locations. Gaussian noise overwhelms the non-Gaussian scalar fluctuations, particularly at the wave numbers which remain after highpass filtering.

IV. DISCUSSION

Scalar PDF's of high-pass-filtered scalar fluctuations in turbulent pipe flow have been examined. When the dominant scalar fluctuations are at length scales well separated from the stirring length scale, the PDF exhibits exponential tails. Otherwise, Gaussian tails are obtained. These results suggest

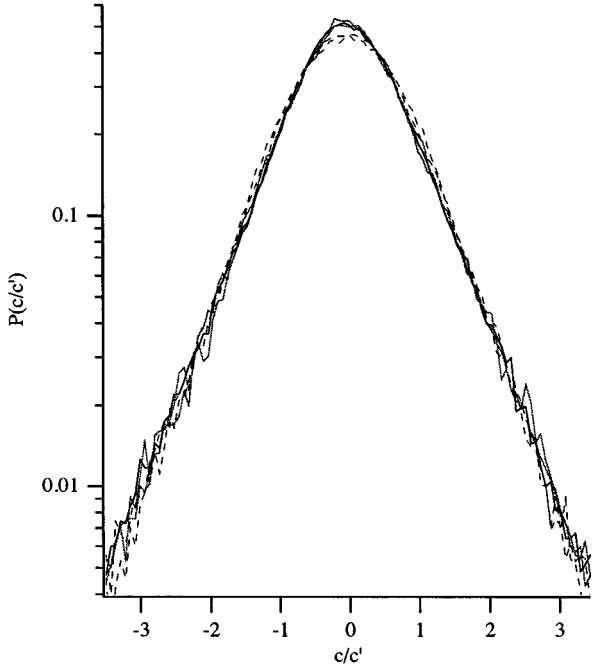

FIG. 10. PDF's of high-pass-filtered ($K=0.27$) data for streamwise locations $x/D=20.5$, 36.0, 50.2, 64.4, and 90.3 (experiment 2). The collapse which is achieved by scaling by the rms indicates self-similarity of the scalar field.

that the high-pass-filtered fluctuations in the former case reflect the mechanism responsible for exponential-tailed PDF's in turbulent flow subject to an imposed mean scalar gradient. The exponential-tailed PDF that is obtained in that case is found to be self-similar.

Previous analysis and measurements suggest that the scale separation leading to these behaviors is a generic property of high-aspect-ratio confined turbulent flows. In these flows, the stirring scale is determined by the duct diameter. Stirring preferentially dissipates the higher-wave-number scalar fluctuations. The remaining low-wave-number fluctuations are then dominant.

In such flows, the present results suggest that scalar fluctuations in the scale range between the dominant scalar fluctuations and the stirring scale may exhibit generic behaviors that are insensitive to details of the flow. In particular, exponential-tailed PDF's may be a more prevalent feature of turbulent mixing than previously recognized.

It is not yet known whether the self-preserving PDF shape identified in this study is likewise generic. Measurements in, e.g., ducts with noncircular cross sections may clarify this point. It would also be interesting to investigate whether other scalar fluctuation properties of the identified mixing regime are generic.

ACKNOWLEDGMENTS

This research was supported by the National Science Foundation under Grant No. CTS 9258445, by the Advanced Combustion Engineering Research Center at the University of Utah and Brigham Young University, and by the Division of Chemical Sciences, Office of Basic Energy Sciences, U.S. Department of Energy.

[1] B. Castaing, G. Gunaratne, F. Heslot, L. Kadanoff, A. Libchaber, S. Thomae, X. Wu, S. Zaleski, and G. Zanetti, J. Fluid Mech. **204**, 1 (1988).
[2] M. Holzer and E. D. Siggia, Phys. Fluids **6**, 1820 (1994).
[3] Jayesh and Z. Warhaft, Phys. Fluids A **4**, 2292 (1992).
[4] B. R. Lane, O. N. Mesquita, S. R. Meyers, and J. P. Gollub, Phys. Fluids A **9**, 2255 (1993).
[5] B. I. Shraiman and E. D. Siggia, Phys. Rev. E **49**, 2912 (1994).
[6] B. I. Shraiman and E. D. Siggia, Physica D **97**, 286 (1996).
[7] J. E. Guilkey, A. R. Kerstein, P. A. McMurtry, and J. C. Klewicki, Phys. Fluids **9**, 717 (1997).
[8] J. E. Guilkey, P. A. McMurtry, and J. C. Klewicki (unpublished).
[9] A. R. Kerstein and P. A. McMurtry, Phys. Rev. E **49**, 474 (1994).
[10] B.R. Ware, D. Cyr, S. Gorti, and F. Lanni, *Measurement of-Suspended Particles by Quasi-Elastic Light Scattering* (Wiley, New York, 1983).
[11] C. J. Lawn, J. Fluid Mech. **48**, 477 (1971).